

The Need for Updated KVN Antenna Efficiencies

by the iMOGABA Team

1 Motivation

The iMOGABA team is currently in the process of analyzing the vast KVN single-dish and VLBI data collected at four frequency bands (22, 43, 86, 129 GHz) from late 2012 to early 2020. Recently (Sang-Hyun Kim, CTA 102), it was noted that the single-dish flux of CTA 102 obtained as part of the iMOGABA program (through cross-scan pointing observations prior to VLBI observation of each source) displayed systematic offsets between the three antennae. In particular, since sometime after 2015B, KUS 22 GHz fluxes were found to be systematically lower than those from the other two stations. This prompted Sang-Hyun Kim (hereafter SHK) to reassess the pre-determined KVN calibration information presented in the KVN status report, with emphasis on the antenna efficiency η_a , where he reported a significant offset between the values in the status report, and those that he found after reanalyzing archive Jupiter observations made with KUS and KTN stations as part of the MOGABA program. After preliminary testing, SHK reported that the new η_a resulted in consistent KUS and KTN single dish fluxes for CTA102

Motivated by this work, Whee Yeon Cheong (hereafter WYC), who was working on 0235+164, re-examined the iMOGABA VLBI data products, and noted that similar systematic offsets were indeed found in the 22 GHz KVN pipeline-calibrated data. 0235+164 is a compact AGN, which is partially resolved at 15 GHz and 43 GHz with the VLBA. Therefore, we expect that 0235+164 will effectively behave like a point-like source in KVN 22 GHz data. However, when examining the correlated flux for each baseline, we see that there are indeed systematic differences between the different baselines. In particular, we find that the flux of the KTN-KYS baselines are 5 to 15 percent higher than the other two baselines throughout the later half of 2015 until the first half of 2018. This is consistent with the report of underestimated KUS single dish fluxes. To check that this wasn't a source-dependent issue, we

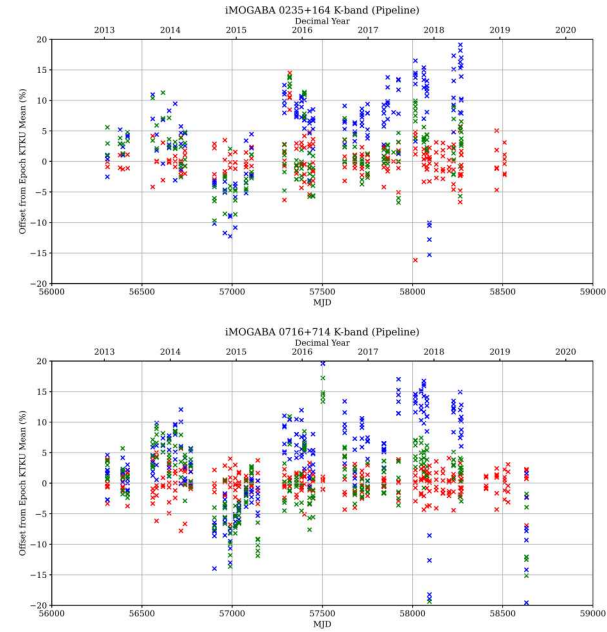


Figure 1: The relative offset per baseline of the 22 GHz correlated flux of 0235+164 and 0716+714 found in the iMOGABA data. Red, green, and blue correspond to KTN-KUS, KUS-KYS, and KTN-KYS baselines respectively. The x-axis is the observation date, both in MJD and in years. The y-axis is the fractional offset with respect to the epoch-mean correlated flux of the KTN-KUS baseline.

also examined the 22 GHz data of 0716+714, which is another compact source, and found similar trends. Therefore, we lean towards the possibility of a systematic amplitude calibration issue, rather than a source-dependent characteristic.

A separate issue that was noted during re-examination of the iMOGABA data was that the KVN gain table provided in the form of ANTAB files was not changed for quite some time. The station gain information is provided in the form of the "degrees per flux unit" (DPFU), and the three coefficients of the 2nd order polynomial gain curve, which depicts the (normalized) dependence of the antenna gain on elevation. The DPFU originates from the equation $S = \frac{2k_B}{A_{eff}} T_a$ which relates the flux density to the measured antenna power. k_B is the Boltzmann constant and $A_{eff} = \eta_a A_{geo}$ is the effective antenna aperture area. Both the KYS and KTN seem to have used the same table since early 2013,

Table 1: KYS GC Table

Band	$DPFU_{max}$	EL_{max}	η_a
K	0.07000711	0	0.55654
Q	0.07529646	41.35	0.59859
W	0.07153217	45.68	0.56866
D	0.04768778	39.73	0.37911

Table 2: KTN GC Table

Band	$DPFU_{max}$	EL_{max}	η_a
K	0.07404062	31.44	0.58861
Q	0.07780584	44.32	0.61854
W	0.06525651	48.74	0.51877
D	0.05019874	49.37	0.39907

while the default gain table of KUS was updated once in early 2016. In table 1, we infer the maximum DPFU of the KYS station (which is reached at an elevation of EL_{max}) and the corresponding η_a from the default GC table. The same is calculated for KTN in table 2. For KUS, we present separate values for before and after the GC table update in table 3 and table 4 respectively.

While it is a known and recommended practice to schedule flux calibrator observations during a VLBI session for the best (relative and absolute) amplitude calibration, here we investigate the degree to which we can calibrate past observations by updating the value of η_a used. In section 2 we describe the process that we took to redetermine the single dish parameters of the three KVN stations. In section 3 we present a brief test of the effect of the newly determined gains on the iMOGABA data.

Table 3: KUS GC Table (pre-update)

Band	$DPFU_{max}$	EL_{max}	η_a
K	0.07843329	21.89	0.62353
Q	0.07717881	19.19	0.61355
W	0.05783313	12.97	0.45976
D	0.03764838	26.31	0.29930

Table 4: KUS GC Table (post-update)

Band	$DPFU_{max}$	EL_{max}	η_a
C	0.07780564	—	0.61854
X	0.06776620	—	0.53872
K	0.07780583	21.89	0.61854
Q	0.07780628	19.19	0.61854
W	0.07153101	49.28	0.56865
D	0.05772760	45.68	0.45892

2 Re-determining KVN antenna efficiencies

We use archive MOGABA cross-scan observations of Jupiter to determine the season-averaged η_a of KTN and KUS. Due to observation conditions, K, Q band observations were typically conducted at KTN and KUS (with center frequencies of 22.4 GHz and 43.1 GHz respectively), while W, D band observations were conducted at KYS. As a first step, here we only consider the K and Q bands. To check for consistency, we attempted two separate analysis on the same data. The first (primarily conducted by SHK) involved analysis of the data with CLASS¹, then use of the pointing-corrected T_a^* of Jupiter and the default KVN η_a calculation code to get the final values. The second approach (primarily conducted by WYC) involved extracting the relevant data from CLASS into python, followed by model-fitting with EMCEE [6] to determine the FWHM, pointing offset, and T_a^* for each AZ/EL scan. The samples created during the production run of the EMCEE analysis were then directly used for calculating the pointing-corrected T_a^* . Note that in this approach, we fit a 1st-order polynomial baseline and 1-dimensional Gaussian simultaneously to the scan data, instead of removing the baseline within CLASS before Gaussian fitting. This was to remove possible systematic effects caused by the window used for baseline removal. We then calculate the distance to Jupiter using the JPL ephemerides (DE430) as implemented in Astropy [1, 2]. Combined with a Jupiter radius of 69911 km, we calculate the angular size of Jupiter at each epoch. Then,

¹<https://www.iram.fr/IRAMFR/GILDAS/doc/html/class-html/class.html>

Table 5: New KTN 22L Parameters

Season	HPBW [†]	η_a^\dagger	η_b^\dagger	η_a^\ddagger	$\frac{\eta_a^\dagger}{\eta_a^\ddagger}$
2015B	122.3	0.642	0.496	0.631	1.02
2016A	121.4	0.626	0.477	0.630	0.99
2016B	—	—	—	—	—
2017A	123.0	0.657	0.513	0.634	1.04
2017B	122.0	0.636	0.490	0.642	0.99
2018A	121.5	0.643	0.491	0.645	1.00
2018B	126.4	0.667	0.548	—	—

[†] : Values determined by WYC.

[‡] : Values determined by SHK.

following [5], we calculate η_a and η_b . For consistency, we use a K-band Jupiter brightness temperature of $T_b = 136.2 \pm 0.85$ K and Q-band brightness temperature of $T_b = 154.8 \pm 0.67$ K from the WMAP seven-year average [4], although there are updated nine-year average brightness temperatures [3] of $T_b = 136.1 \pm 0.75$ K and $T_b = 154.3 \pm 0.59$ K respectively (albeit, at slightly different center frequencies). In both analysis attempts, for simplicity, we assume a flat gain curve for both frequency bands.

The season-averaged results from 2015B to 2018B for KTN and KUS are presented from table 5 to table 8. KVN seasons not presented here were either left out at this stage of the analysis, or had insufficient observational data of Jupiter within the MO-GABA program. We find that the results obtained by SHK using the standard KVN calibration code and that obtained by WYC using a custom code are consistent with each other to within a few percent, suggesting that there is no significant issue with the custom code used by WYC.

Before continuing, we make a few comments about individual stations. We find that the 22 GHz η_a of KTN is approximately 0.64 from 2015B to 2018A. This is $\sim 9\%$ greater the default value within the KVN ANTAB files. At 43 GHz, there seems to be a systematic shift between 2016A and 2016B, although it is difficult to pinpoint the exact month, due to a lack of data between May of 2016 to January of 2017 (note that we have categorized the observation on January 13, 2017 as part of the 2016B season). The average η_a of KUS at 22 GHz is approximately 0.56, which is 10% less than the ANTAB value. We

Table 6: New KTN 43L Parameters

Season	HPBW [†]	η_a^\dagger	η_b^\dagger	η_a^\ddagger	$\frac{\eta_a^\dagger}{\eta_a^\ddagger}$
2015B	62.05	0.607	0.447	0.599	1.01
2016A	62.29	0.596	0.442	0.597	1.00
2016B	60.53	0.684	0.479	0.688	0.99
2017A	60.92	0.668	0.474	0.650	1.03
2017B	61.90	0.640	0.469	0.641	1.00
2018A	61.88	0.654	0.479	0.652	1.00
2018B	62.18	0.574	0.424	—	—

[†] : Values determined by WYC.

[‡] : Values determined by SHK.

Table 7: New KUS 22L Parameters

Season	HPBW [†]	η_a^\dagger	η_b^\dagger	η_a^\ddagger	$\frac{\eta_a^\dagger}{\eta_a^\ddagger}$
2015B	121.7	0.553	0.423	0.557	0.99
2016A	121.5	0.561	0.428	0.563	1.00
2016B	122.5	0.567	0.439	0.571	0.99
2017A	122.0	0.565	0.434	0.569	0.99
2017B	121.5	0.540	0.412	0.551	0.98
2018A	121.5	0.560	0.427	0.566	0.99

[†] : Values determined by WYC.

[‡] : Values determined by SHK.

Table 8: New KUS 43L Parameters

Season	HPBW [†]	η_a^\dagger	η_b^\dagger	η_a^\ddagger	$\frac{\eta_a^\dagger}{\eta_a^\ddagger}$
2015B	62.06	0.578	0.426	0.582	0.99
2016A	61.67	0.638	0.464	0.621	1.03
2016B	63.03	0.654	0.496	0.651	1.00
2017A	61.53	0.653	0.472	0.640	1.02
2017B	61.61	0.611	0.443	0.607	1.01
2018A	61.56	0.651	0.471	0.639	1.02

[†] : Values determined by WYC.

[‡] : Values determined by SHK.

have yet to check whether this is the case for earlier dates as well (although figure 1 suggests that this issue does start since 2015B). At 43 GHz, there is a significant increase of η_a between 2015B and 2016A. Looking at the individual data, this seems to have occurred between January 1st and March 12th of 2016.

As mentioned at the start of this section, there is limited K,Q band MOGABA data observed at KYS. However, there are indications that the η_a of KYS also varies during this period. The first indication comes from re-calibration of the iMOGABA correlated fluxes using the new KTN and KUS η_a . With the assumption that the gain curve of the three stations at K-band is flat enough to simply scale the correlated flux, we may re-calibrate the data without re-running them through the pipeline. Jupiter observations were part of iMOGABA observations during the 2013A season, and corrections are already applied for all three stations. Therefore, we do not modify these observations. For observations made from 2013B to 2015A, we use the values of η_a presented in the online KVN status report. From 2015B to 2018A, we use the newly determined values of η_a for KTN and KUS. At this stage, we do not correct for KYS. The results are presented in figure 2. Compared to figure 1, we find that there is noticeable reduction of the systematic offsets between different baselines. However, the KUS-KYS (green), and KTN-KYS (blue) baselines are still offset during some seasons by 5% to 10%. This indicates that there is a systematic calibration issue with the KYS station as well (at least at 22 GHz).

The second indication comes from the single-dish pointing observations made as part of iMOGABA observations. We compare the pointing-corrected 22 GHz and 43 GHz T_a^* measurements of 3C 84 made with KUS and KYS. We find that the KYS 43 GHz T_a^* is significantly reduced during 2016B and 2017A. There also seems to be a linear variation of the relative gain at 22 GHz during the same time period. We also note that there is a significant shift in the 22 GHz relative gain between 2018A and 2018B, although this period is not of our immediate interest. All in all, we find that both of these points justifies an investigation of the KYS η_a as well.

Due to the lack of K, Q band MOGABA observations at KYS, we turn to archive Jupiter obser-

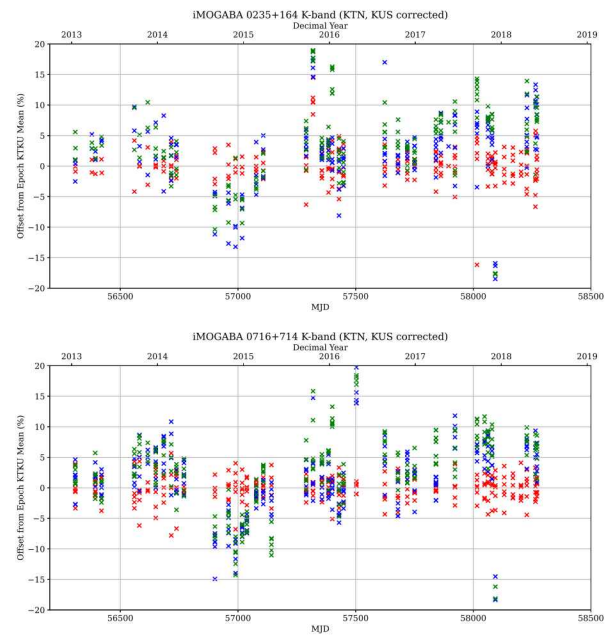


Figure 2: The relative offset per baseline of the 22 GHz correlated flux of 0235+164 and 0716+714 found in the iMOGABA data after re-scaling of the visibilities with the new η_a of KTN and KUS. Red, green, and blue correspond to KTN-KUS, KUS-KYS, and KTN-KYS baselines respectively. The x-axis is the observation date, both in MJD and in years. The y-axis is the fractional offset with respect to the epoch-mean correlated flux of the KTN-KUS baseline.

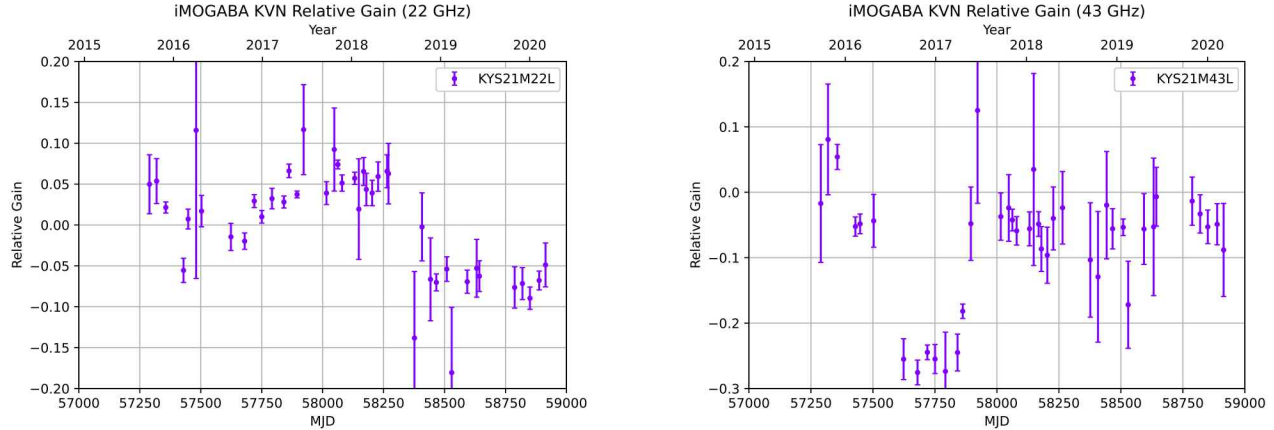


Figure 3: The deviation of the ratio of T_a^* of KYS with respect to that of KUS from unity. The values of T_a^* within a single iMOGABA epoch were averaged, with the error-bars calculated from either the standard deviation of the measured T_a^* if multiple scans were available, or from the 1-sigma confidence limits calculated from EMCEE if only a single (good) scan was available.

vations made outside of the MOGABA program. Such observations include gain curve observations made by the KVN operation team, as well as observations conducted by individual projects. Due to the vast number of data, we use the semi-automatic code used by WYC for KTN and KUS, which we have shown to be consistent with the conventional method. As with KTN and KUS, we assume a flat gain curve at both frequencies. The results are summarized in table 9 and table 10. Note that unlike KTN and KUS, the data used for KYS have different center frequencies. At 22 GHz, it is generally at either 21.7 GHz or 22.2 GHz. For consistency with the results for KTN and KUS, we use observations at 22.2 GHz when available. There are some seasons where this is not possible, in which case we use observations at 21.7 GHz. The mean frequency of the data used is also presented in units of GHz.

We see that the newly determined parameters of KYS generally follows the trends presented in figure 3. In particular, we note that the significant dip in the 43L gain of KYS during 2016B and 2017A is also present in the results in table 10. Looking at the individual observations, $\eta_a \approx 0.5$ since October 4th, 2016. It remains at this level until at least May 14th, 2017. On the next available observation, which was on May 19th, 2017, we find $\eta_a \approx 0.64$. The fitted HPBW is also larger than expected during this period, although we have yet to cross-check

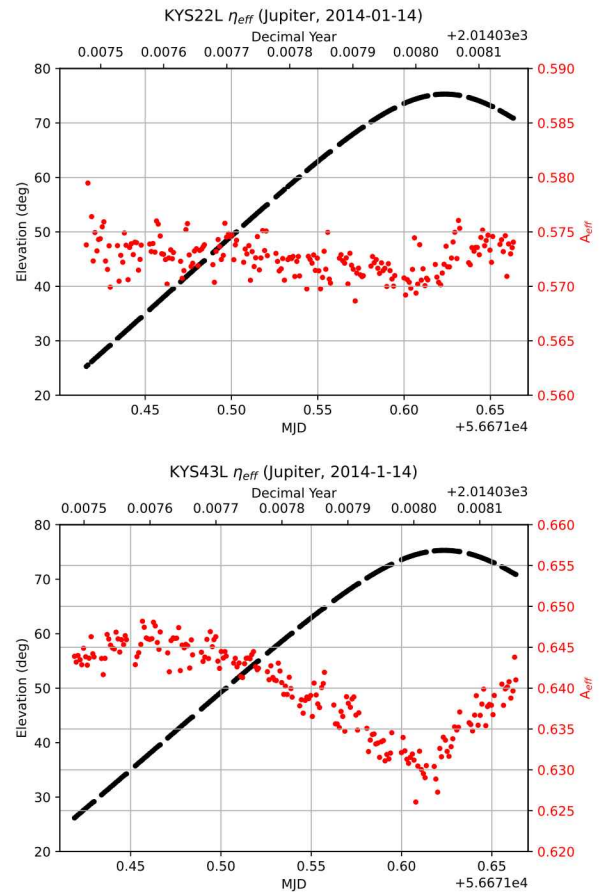


Figure 4: Example of the fit results for KYS at 22 GHz and 43 GHz. This specific data was part of gain curve measurements made on January 14th, 2014.

Table 9: New KYS 22L Parameters

Season	FREQ	HPBW	η_a	η_b
2013A	22.2	122.7	0.568	0.435
2013B	22.3	123.1	0.583	0.451
2014A [†]	22.3	122.8	0.586	0.453
2014B [‡]	21.7	126.3	0.568	0.439
2015A	22.3	122.3	0.569	0.434
2015B [†]	22.3	126.0	0.567	0.450
2016A [†]	21.7	125.4	0.534	0.408
2016B	21.7	127.3	0.573	0.449
2017A	22.3	122.2	0.593	0.452
2017B	22.2	129.3	0.635	0.540
2018A [†]	22.2	126.6	0.603	0.491

† : Small number of Jupiter observations.

‡ : η_a may be over-estimated (see section 4)

Table 10: New KYS 43L Parameters

Season	FREQ	HPBW	η_a	η_b
2013A	42.9	61.89	0.652	0.474
2013B ¹	43.2	64.84	0.493	0.398
2013B ²	43.2	61.82	0.630	0.462
2014A	43.2	61.79	0.644	0.473
2014B	43.5	61.57	0.604	0.446
2015A	43.2	61.32	0.635	0.458
2015B [†]	43.2	61.79	0.587	0.430
2016A	43.1	61.01	0.581	0.414
2016B [‡]	42.6	69.59	0.471	0.426
2017A ^{3‡}	43.2	67.54	0.502	0.439
2017A ^{4‡}	43.2	64.67	0.638	0.511
2017B	43.1	65.59	0.637	0.524
2018A	43.2	64.13	0.630	0.496
2018B	43.6	65.67	0.627	0.525
2019A [†]	43.1	63.65	0.636	0.493
2019B [†]	43.1	65.80	0.628	0.519
2020A [†]	43.0	66.53	0.618	0.520
2020B [†]	43.1	63.17	0.667	0.508

† : Small number of Jupiter observations.

‡ : Largely different values.

1 : Before August 14th, 2013

2 : After August 28th, 2013

3 : Before May 15th, 2017

4 : After May 18th, 2017

with other data (for example, iMOGABA cross-scan observations) to see if this is actually the case. We note that there was a brief period in 2013 where the KYS 43L η_a values were at a similar level. A series of Jupiter observations made from August 10th to August 13th of 2013 also displayed significantly lower η_a and a slightly larger HPBW compared to the typical values before and after these observations.

3 Effect of updated antenna efficiencies

First, we investigate the final outcome of recalibrating the iMOGABA K-band correlated flux with the new η_a . The results are presented in figure 5. We see that with the addition of KYS corrections, the majority of season-averaged systematic offsets between baselines are eliminated. Compared to just KTN and KUS corrections (figure 2), there is a significant reduction of the systematic offset of KYS baselines, particularly for observations made in 2017 and later. All in all, we find that after applying all corrections, the correlated flux of all three baselines are typically consistent on the level of $\pm 5\%$.

We also expect improvements in the KVN VLBI imaging as well. We proceed with imaging analysis of the iMOGABA9 data (which was observed between November 19th and 20th of 2013) with DIFMAP. We CLEAN both the current pipeline output, and the newly calibrated data. We use natural weighting (uvweight 0,0 in DIFMAP). We first average the data by 10 seconds. Then, we proceed with flagging (of course, applying the same data flagging for both the pipeline and newly calibrated datasets) and initial self calibration with "startmod". Afterwards, we conduct multiple rounds of CLEAN and phase self-calibration. For comparison, we use the dynamic range (hereafter DR) of the final image as a measure of the image quality. The results are presented in table 11. We also present the CLEAN image of a few selected sources in figure 6. Overall, we find that the RMS of the residual image is noticeably reduced with the new η_a applied. The peak of the CLEAN image is comparable in both cases, resulting in a general improvement of the DR. We note that only a single scan of 1127-145 was observed during iMOGABA9. Generally, such sources

Table 11: iMOGABA9 DR Comparison

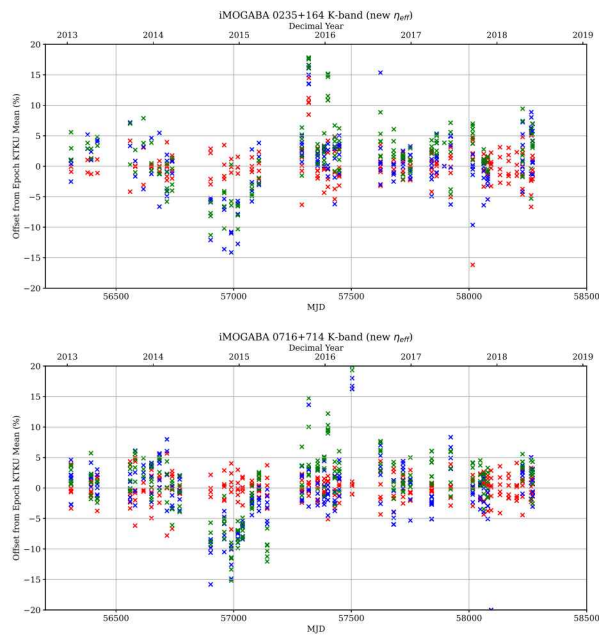


Figure 5: The relative offset per baseline of the 22 GHz correlated flux of 0235+164 and 0716+714 found in the iMOGABA data after re-scaling of the visibilities with the new η_a of all three stations. Red, green, and blue correspond to KTN-KUS, KUS-KYS, and KTN-KYS baselines respectively. The x-axis is the observation date, both in MJD and in years. The y-axis is the fractional offset with respect to the epoch-mean correlated flux of the KTN-KUS baseline.

Source	Pipeline			New η_a		
	S_{peak} [$\frac{\text{Jy}}{\text{b}}$]	RMS [$\frac{\text{mJy}}{\text{b}}$]	DR	S_{peak} [$\frac{\text{Jy}}{\text{b}}$]	RMS [$\frac{\text{mJy}}{\text{b}}$]	DR
4C +28.07	2.79	17.6	159	2.78	14.9	186
0235+164	0.851	13.6	62.4	0.848	12.0	70.5
3C 84	24.0	161	149	23.9	142	168
3C 111	3.92	26.4	149	3.90	17.0	229
0420-014	5.00	76.7	65.2	4.98	48.2	103
0528+134	1.16	4.53	255	1.15	3.79	303
0716+714	2.50	18.9	132	2.49	10.8	230
J0730-1141	3.71	39.7	93.4	3.69	17.9	206
0735+178	1.01	3.30	305	1.00	3.92	255
0827+243	0.876	14.3	61.3	0.873	11.3	77.0
0836+710	1.64	7.67	214	1.63	5.43	301
OJ 287	4.71	16.4	288	4.68	15.2	309
4C +39.25	7.88	52.9	149	7.85	37.2	211
1055+018	2.85	16.8	170	2.85	7.48	381
Mrk 421	0.434	1.61	270	0.433	1.39	312
1127-145†	2.34	4.31	544	2.32	2.49	933
1156+295	0.856	18.5	46.3	0.852	14.5	58.9
1222+216	2.26	13.6	166	2.27	9.52	238
M87	1.85	10.8	172	1.86	4.14	449
3C 279	26.0	204	127	25.8	116	223
1308+326	1.47	10.3	142	1.46	5.89	248
3C 286	0.394	19.0	20.7	0.358	9.83	36.4
1343+451	0.826	6.90	120	0.823	5.27	156
1611+343	3.29	28.3	116	3.27	19.7	166
4C +38.41	5.11	33.0	155	5.10	23.1	221
3C 345	4.21	31.3	135	4.15	28.4	146
1749+096	2.80	20.5	137	2.78	11.9	234
1921-293	7.43	91.8	80.9	7.45	33.8	220
BLLAC	4.52	24.9	181	4.50	19.5	231
3C 446	2.23	9.05	246	2.22	6.38	348
CTA 102	2.08	13.2	157	2.08	10.6	196
3C 454.3	5.95	26.9	221	5.92	16.8	353

† : Likely over-CLEANed (see text for details)

were CLEANed with a single point source. However, for 1127-145, there is a significant offset of the closure phase from zero, suggesting the existence of source structure. Therefore, we conducted additional CLEANing along the known jet direction of this source. It is likely that this resulted in excessive CLEANing and an overestimation of the DR.

The initial amplitude calibration of iMOGABA9 was already good (approximately 5% offset of KYS baselines). We briefly examine the effect of the re-calibration on a few select targets from iMOGABA48, which was conducted between November 4th and 5th of 2017. The partial results are summarized in table 12 and figure 7. Since this was an

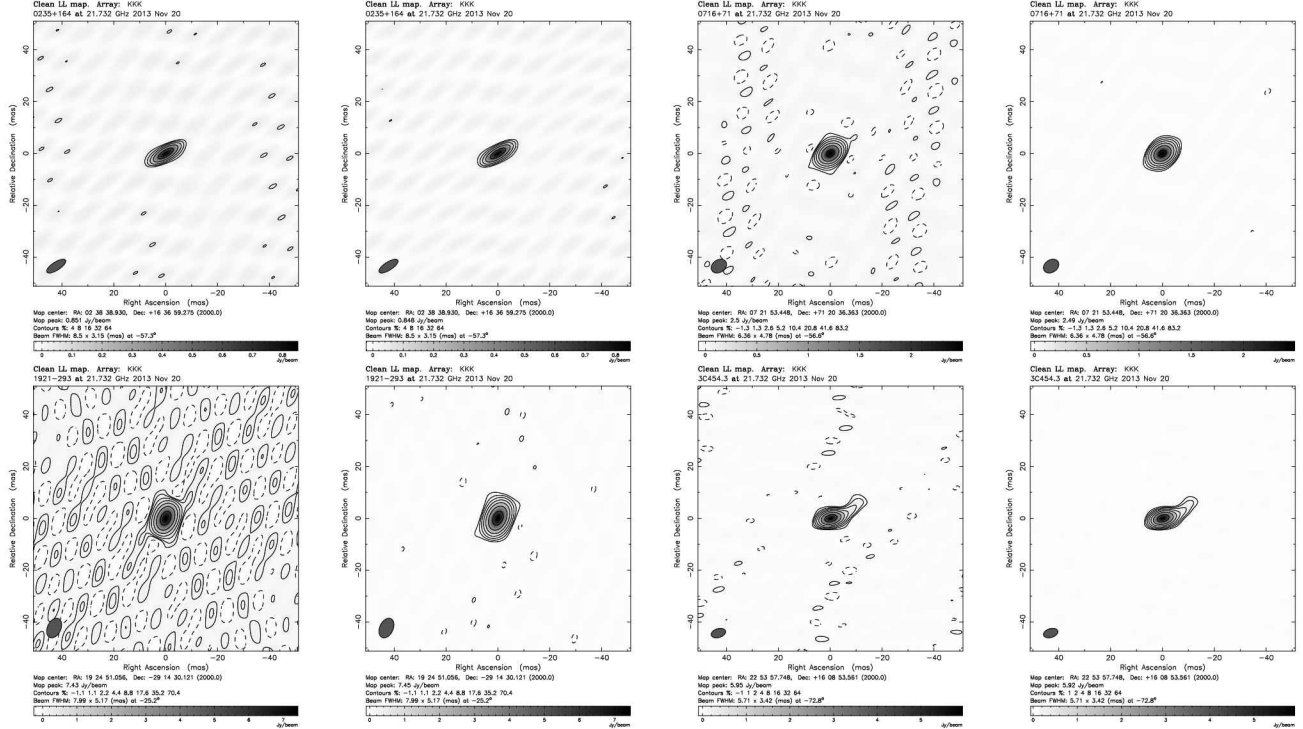


Figure 6: iMOGABA9 CLEAN images of 0235+164, 0716+714, 1921-293, and 3C 454.3. For each set, the image on the left was made using the pipeline data, while the image on the right was made from the newly calibrated data.

epoch where it seems both KTN and KYS η_a were underestimated, while KUS η_a was overestimated, we find a slight decrease in the overall peak flux density for all four tested sources. However, there is a **very** significant improvement in the residual RMS. In particular, the VLBI images from the pipeline data contain significant, symmetric side lobes, which are indications of amplitude calibration errors. In fact, the strong residual pattern made it impossible to locate the faint North-East jet structure of 1921-293 at all with the pipeline data. Re-calibration of the pipeline data allowed us to successfully CLEAN the faint jet structure of 1921-293 as well (although it is not apparent in the CLEAN image, due to the “core-dominated flux” nature of this source).

4 Remaining Issues

Despite the positive results from the limited number of tests that we conducted, there are still some points of concern remaining. Although we have tested with correlated data, a full test to

Table 12: iMOGABA48 DR Comparison

Source [†]	Pipeline			New η_a		
	S_{peak} [Jy b]	RMS [mJy b]	DR	S_{peak} [Jy b]	RMS [mJy b]	DR
0235+164	1.33	12.1	109	1.29	5.00	259
0716+714	2.37	23.8	99.4	2.31	7.49	308
1921-293	6.49	94.4	68.7	6.39	38.1	168
3C 454.3	14.8	107	139	14.3	32.3	444

† : Only a subset of the full source list was tested.

check the consistency of the **single-dish** cross-scan data from the three stations is still required. In particular, we determined season-averaged η_a , while there may be systematic variations from observation-to-observation within a single KVN season as well (for example, between MJD 57500 and MJD 58000 of the upper plot in figure 3). We have also yet to fully evaluate the dependence of the gain with elevation. However, past observations suggest that the variation of η_a with elevation is only a few percent for 22 and 43 GHz observations.

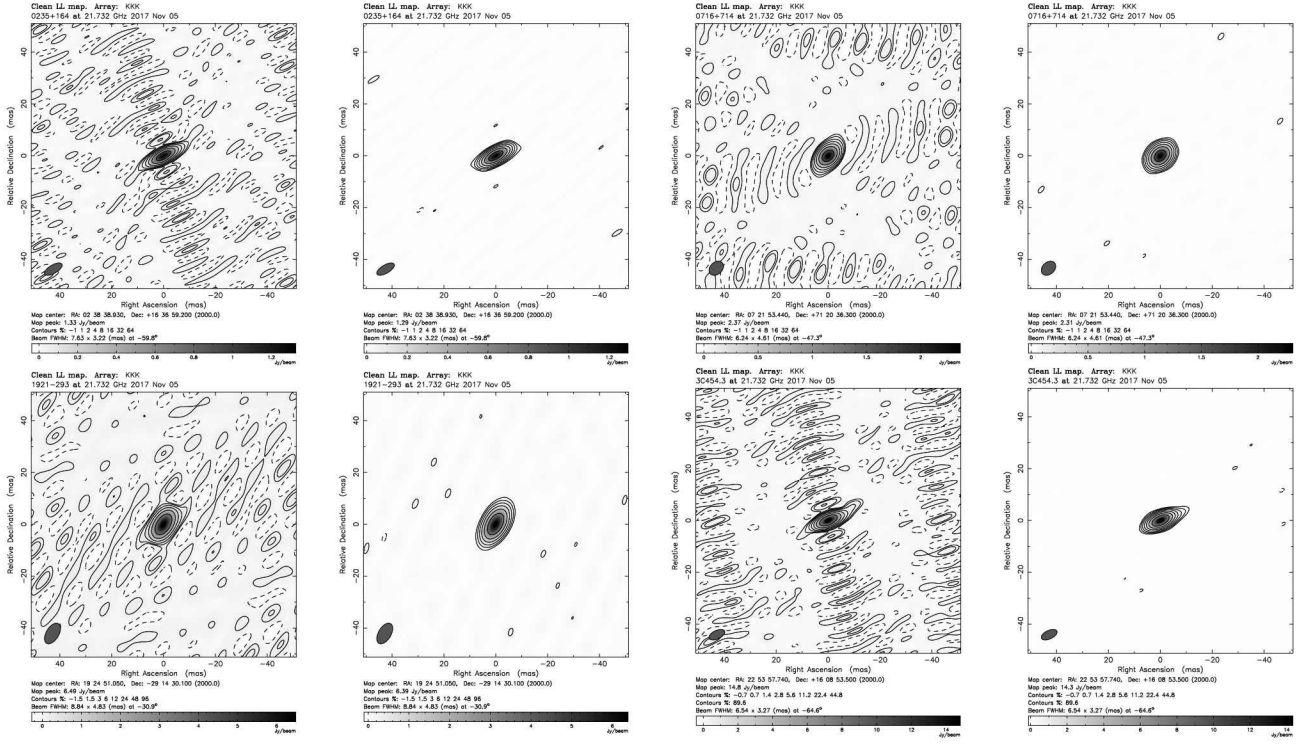


Figure 7: iMOGABA48 CLEAN images of 0235+164, 0716+714, 1921-293, and 3C 454.3. For each set, the image on the left was made using the pipeline data, while the image on the right was made from the newly calibrated data.

This may be greater than 10 percent for 86 and 130 GHz, which is why we did not include them in this analysis.

Even after re-calibration, we find that the correlated flux of the KYS baselines are still systematically low by 5 to 10 percent during the 2014B season. The available Jupiter observations at KYS were carried out on November 10th, 2014 and January 10th, 2015, both of which were at 21.7 GHz (instead of the standard 22.4 GHz). There is the possibility that the difference in frequency is the cause of the underestimation of η_a during this season. The ratio-square of the wavelength of the two frequencies is approximately 7%. However, we do not find similar trends for observations in 2016A and 2016B, where we also used Jupiter observations made at 21.7 GHz. We may attempt to see if there is additional data of different planets to cross-check the results from Jupiter, or we may test with standard flux calibrators (such as 3C 286, although this source does display some inherent flux variation at 22 GHz). Of course, we may need to check the η_a of KTN and KUS, for which it was already shown that the KVN status report values may be different from the actual values. However, the fact that both KYS baselines are offset by roughly equivalent levels suggests that the problem is with the KYS station.

Apart from the overall amplitude calibration issues, there are two large time-spans where the K-band correlated flux of both KVNYS baselines are low by more than 20%. The first is from December 6th, 2017 to March 26th, 2018 (iMOGABA50 to iMOGABA55), and the second is from October 16th, 2018 to February 15th, 2019 (iMOGABA60 to iMOGABA64). This does not seem to be a gain-calibration issue, as the relative single-dish observations between KUS and KYS does not vary to this extent. At this point in time, this issue also seems to be isolated to K-band observations, although a thorough check (including re-determination of η_a at higher frequencies) is required to be sure. We could attempt to manually calibrate the data in these periods by determining the overall scaling factor with multiple compact sources. However, we find it important to determine the root cause of the problem as well.

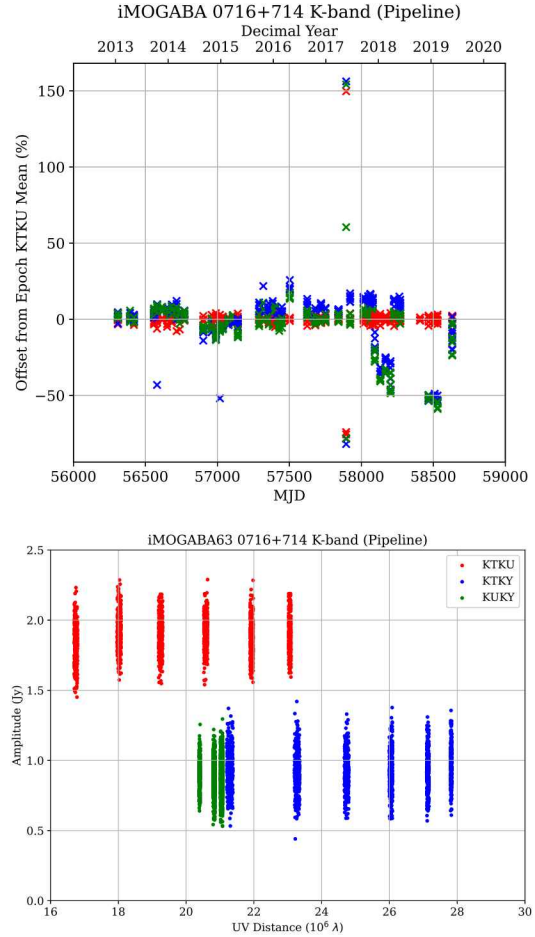


Figure 8: The relative offset per baseline of the 22 GHz correlated flux of 0716+714 found in the iMOGABA pipeline-calibrated data showing significant offset of the KYS baselines. The "radplot" of the iMOGABA63 data is presented as an example.

5 Conclusion

We report the finding of significant variation of the η_a of the KVN stations, the effects of which are present in both single dish observations and VLBI observations. The effect is particularly prominent since KVN 2015B season for KTN and KUS observations. Through past MOGABA observations of Jupiter, we have re-determined the values of η_a for KTN and KUS at 22.4 GHz and 43.1 GHz from KVN seasons 2015B to 2018B. We have also attempted to correct for KYS as well from archive Jupiter observations, although there are remaining issues for certain KVN seasons. After re-calibration with the newly found η_a for all three stations, we find that both the inter-baseline and scan-to-scan flux of a single baseline are typically consistent to $\pm 5\%$. Preliminary imaging tests with select iMOGABA data indicates an improvement in the DR of the final image for both compact and extended sources, at a wide range of declination. Despite these positive results, there are remaining issues (particularly with KYS) that may not be limited to the value of η_a , which we will work to resolve in the future.

References

- [1] Astropy Collaboration. Astropy: A community Python package for astronomy. *Astronomy & Astrophysics*, 558:A33, Oct. 2013.
- [2] Astropy Collaboration. The Astropy Project: Building an Open-science Project and Status of the v2.0 Core Package. *The Astronomical Journal*, 156(3):123, Sept. 2018.
- [3] C. L. B. et al. NINE-YEAR WILKINSON MICROWAVE ANISOTROPY PROBE (WMAP) OBSERVATIONS: FINAL MAPS AND RESULTS. *The Astrophysical Journal Supplement Series*, 208(2):20, sep 2013.
- [4] J. L. W. et al. SEVEN-YEAR WILKINSON MICROWAVE ANISOTROPY PROBE (WMAP) OBSERVATIONS: PLANETS AND CELESTIAL CALIBRATION SOURCES. *The Astrophysical Journal Supplement Series*, 192(2):19, jan 2011.
- [5] S.-S. L. et al. Single-dish performance of KVN 21 m radio telescopes: Simultaneous observations at 22 and 43 GHz. *Publications of the Astronomical Society of the Pacific*, 123(910):1398–1411, dec 2011.
- [6] Foreman-Mackey et al. emcee: The MCMC Hammer. *Publications of the Astronomical Society of the Pacific*, 125(925):306, Mar. 2013.

Document Version Info

Date	Description
210506	First version, Submitted to KVN AOC.
210511	Typo fix, Wording fix. Add all IM9 CLEAN images. Edit CLN image of Mrk421.
210517	Added IM32 CLEAN images.
210527	Updated KUS,KTN table values to incorporate deconvolution with Jupiter size. Updated KYS22L table values to incorporate deconvolution with Jupiter size.
210528	Updated KYS43L table values to incorporate deconvolution with Jupiter size. Updated some portions of text for better clarity.
Current	Reanalyzing VLBI images to account for updates to η_a made since the initial version.

ToDo List

- Need to update VLBI CLEAN image figures to incorporate changes to the tables caused by the addition of deconvolving the fitted FWHM with the Jupiter size before pointing correction, etc. Note that the changes to the 22 GHz η_a values are not too large, so the results shouldn't change too much.
- Even after the above corrections, there are remaining offsets between the single-dish flux measurements made between KVNYS and KVNU (based on the iMOGABA pointing observations). Also, KYS Jupiter observation frequencies are all over the place. We either need to check with a separate flux calibrator (other planets, 3C 286, etc) or consider a new calibration method. Overall, KVNU seems to be stable at 22 and 43 GHz. Therefore, currently considering a new calibration scheme where we take

the $T_a^*(\text{EL})$ of all of the sources measured at the three stations for a single iMOGABA epoch. Then attempt to find a global solution of T_a^* (which should be the same at all stations), and a 2nd order polynomial gain curve for each station (which should be the same for all sources). The absolute amplitude degeneracy is solved by normalizing the gain curve peak of the reference station to 1. Absolute amplitude calibration is then conducted using MOGABA observations of the reference station.

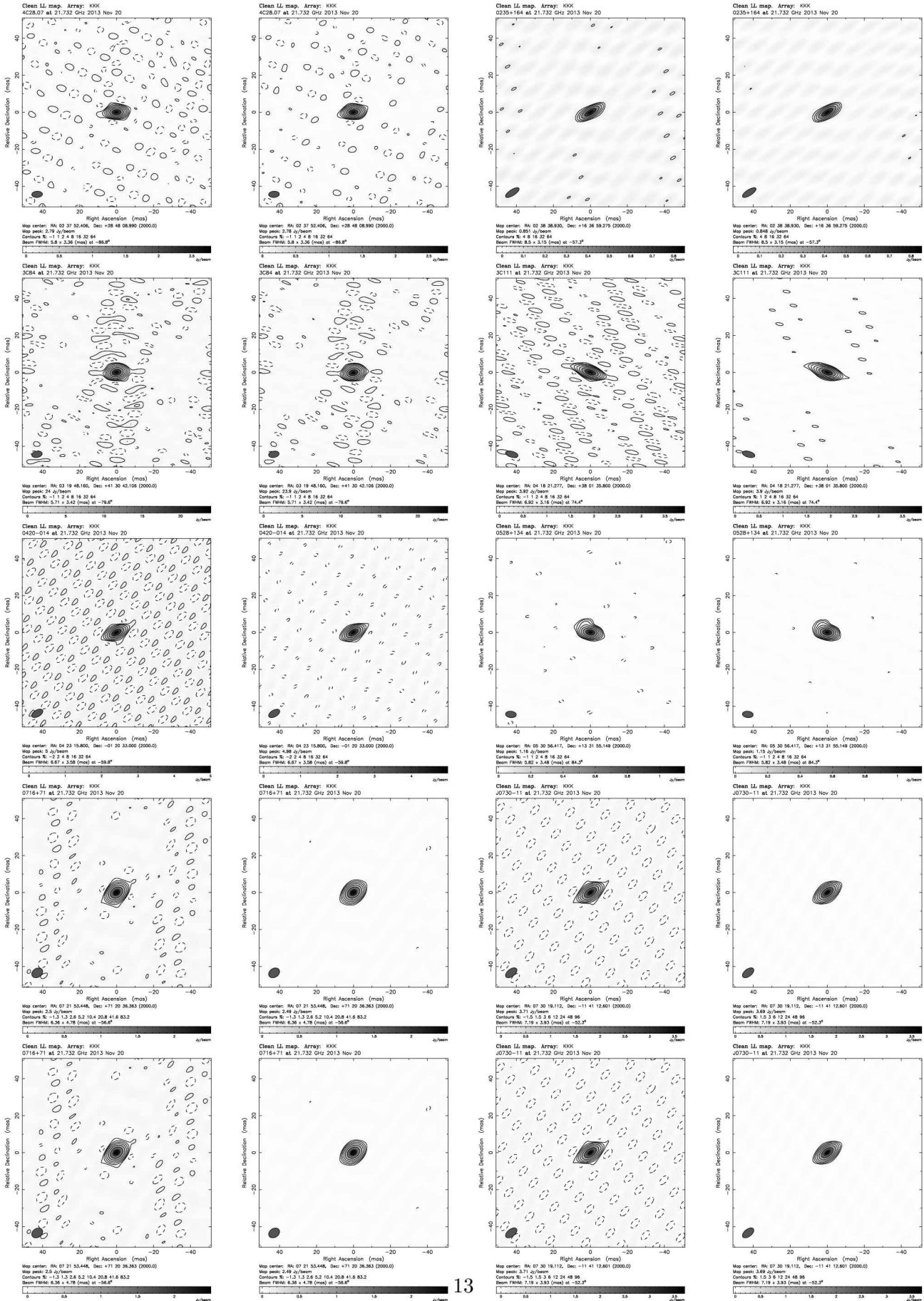


Figure 9: iMOGABA9 CLEAN images. For each set, the image on the left was made using the pipeline data, while the image on the right was made from the newly calibrated data.

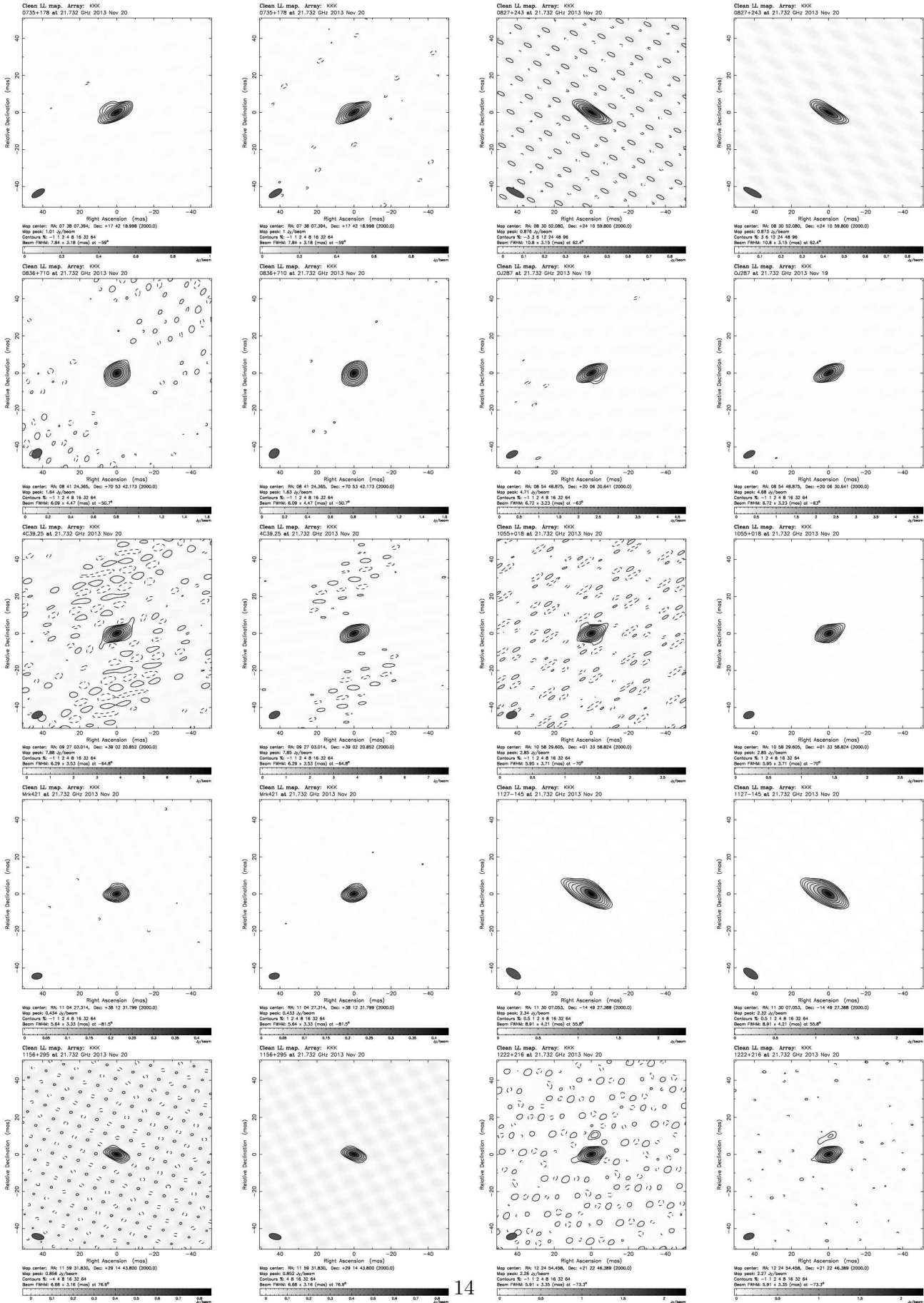


Figure 10: iMOGABA9 CLEAN images. Continued

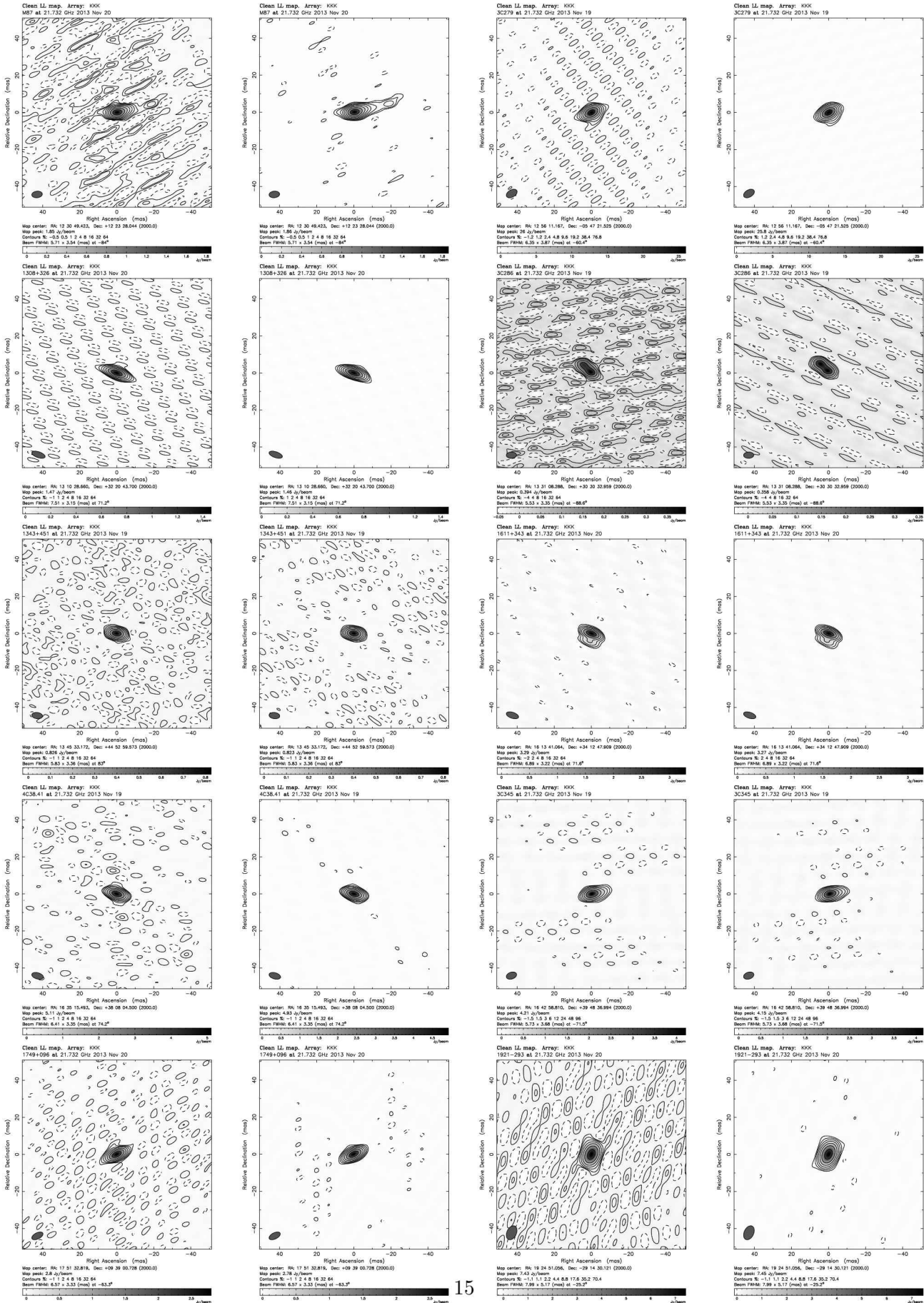


Figure 11: iMOGABA9 CLEAN images. Continued

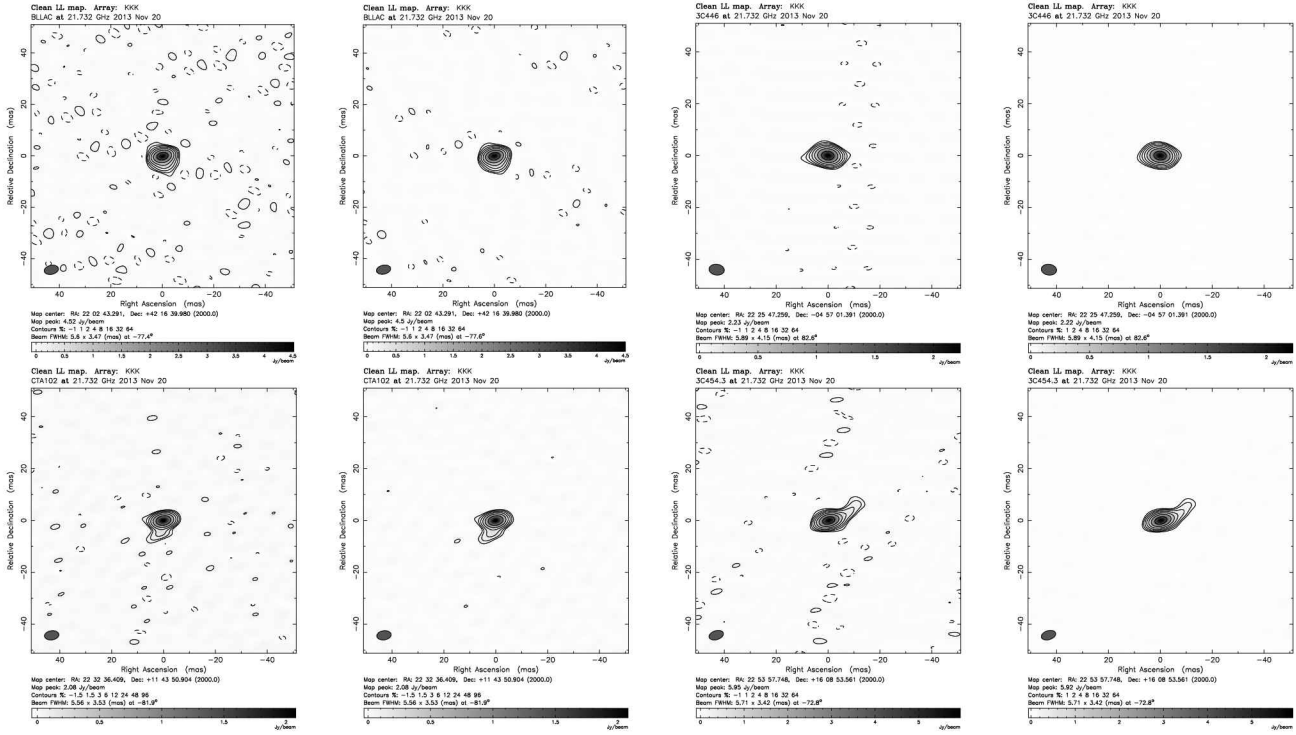


Figure 12: iMOGABA9 CLEAN images. Continued

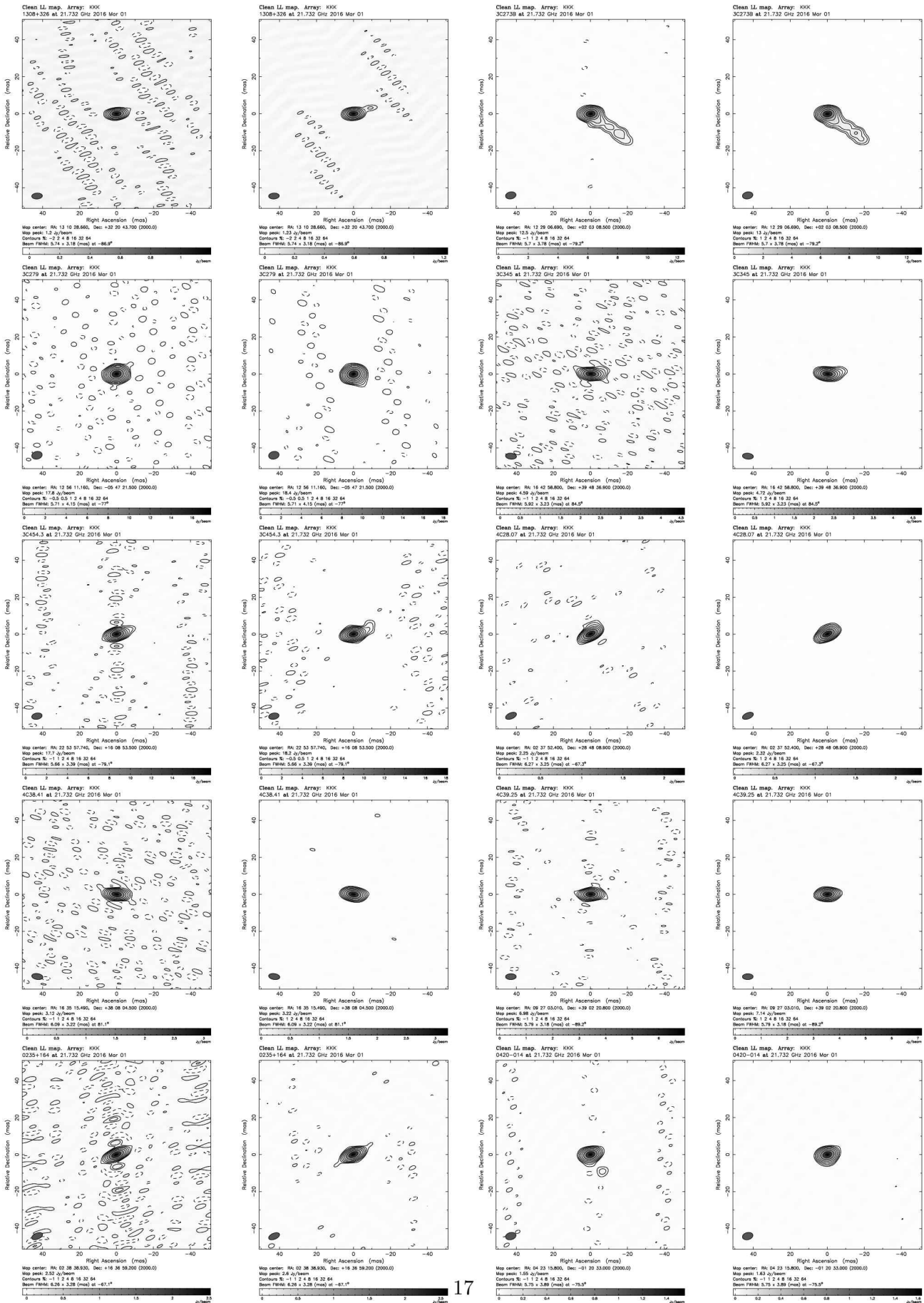


Figure 13: iMOGABA32 CLEAN images. For each set, the image on the left was made using the pipeline data, while the image on the right was made from the newly calibrated data.

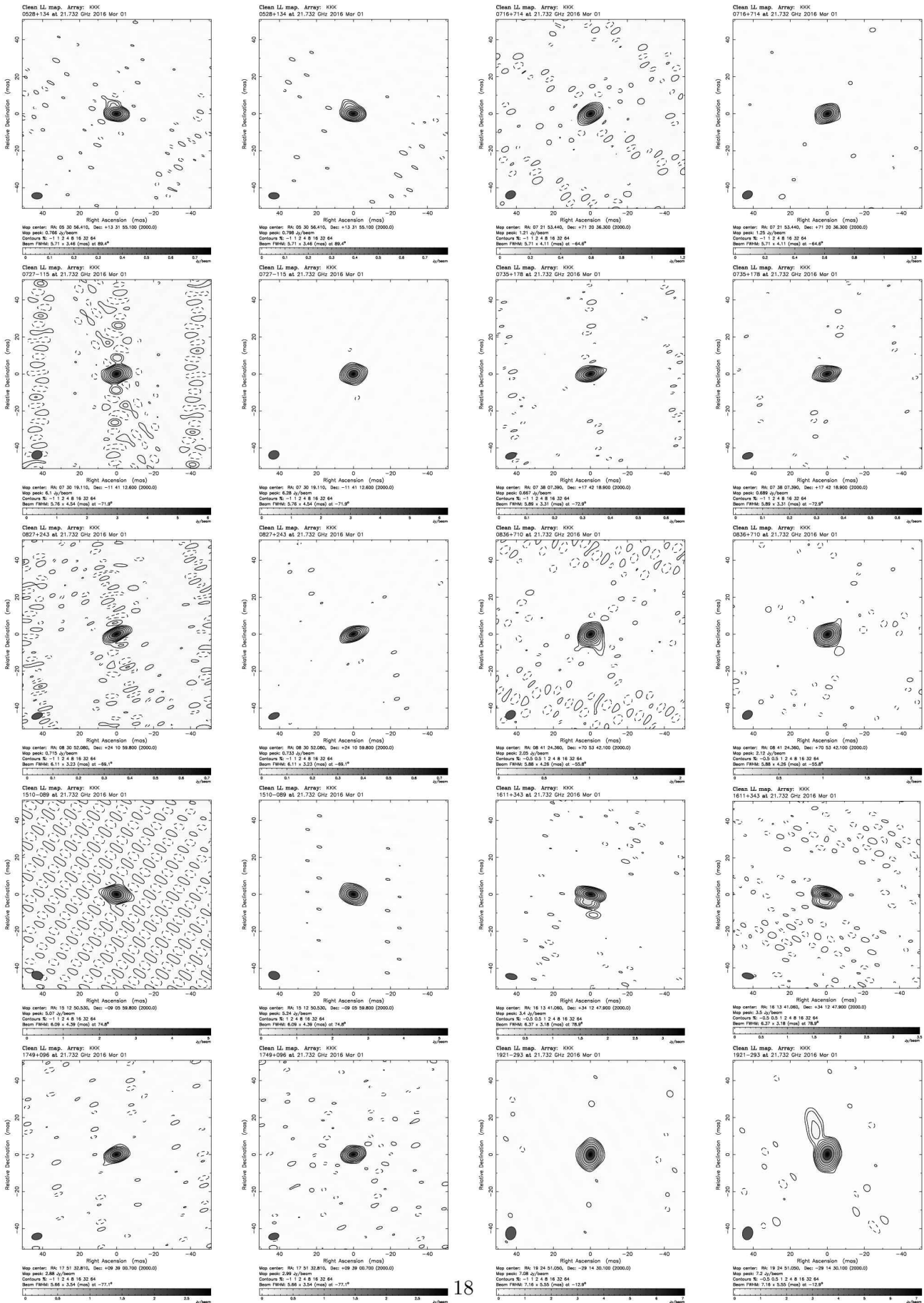


Figure 14: iMOGABA32 CLEAN images. Continued

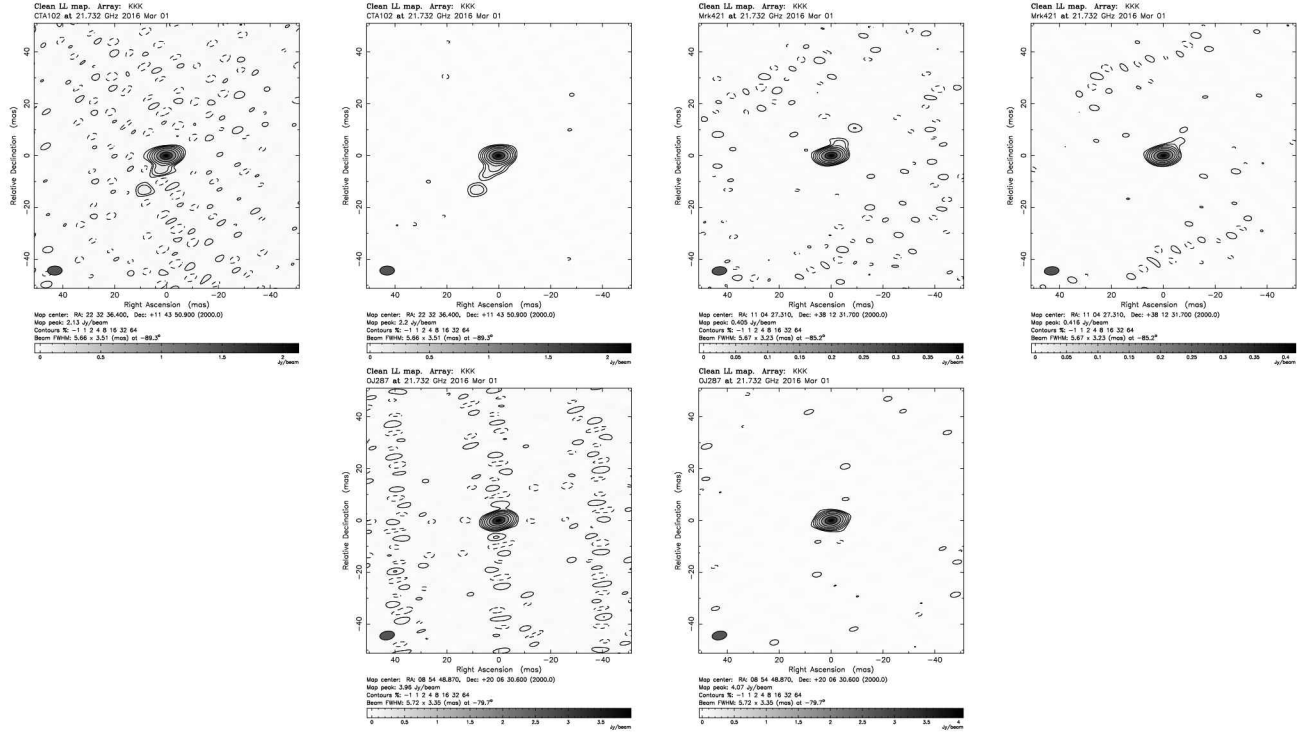


Figure 15: iMOGABA32 CLEAN images. Continued